Rydberg−Valence Mixing in the Carbon 1s Near-Edge X-ray Absorption Fine Structure Spectra of Gaseous Alkanes

Stephen G. Urquhart* and Rob Gillies

Department of Chemistry, 110 Science Place, Saskatoon, Saskatchewan S7N 5C9, Canada

Received: October 11, 2004; In Final Form: January 8, 2005

We have acquired high-resolution carbon 1s near-edge X-ray absorption fine structure (NEXAFS) spectra of methane, ethane, propane, isobutane, and neopentane. These experimental measurements are complemented by high-quality ab initio calculations, performed with the improved virtual orbital approximation. The degree and character of Rydberg−valence mixing in the preedge of the NEXAFS spectra of these species is explored. Significant Rydberg−valence mixing only occurs when there are excited states of valence σ^*(C−H) character that have the appropriate symmetry to interact with excited states of Rydberg character. Our results show that this mixing is only present when there are C−H bonds to the core excited carbon atom.

1. Introduction

The high-resolution carbon 1s near-edge X-ray absorption fine structure (NEXAFS) spectra of gaseous alkanes are dominated by a distinct series of carbon 1s → Rydberg transitions that converge to the ionization potential.[1−5] In contrast, preedge features in the carbon 1s NEXAFS spectra of *condensed* alkanes such as Langmuir−Blodgett[6] and self-assembled[7−9] monolayers and polyethylene[10,11] are much broader than preedge features in the spectra of *gaseous* alkanes. These broad features have traditionally been assigned as carbon 1s → σ^*(C−H) valence transitions.[6,10] However, Bagus and Wöll have argued that these states are predominately of Rydberg character in the condensed alkanes, even though Rydberg states are expected to be attenuated in the solid phase.[12,13] We wish to obtain a precise understanding of the nature of Rydberg−valence mixing in condensed alkanes, in part to improve the analytical utility of NEXAFS spectra for chemical microanalysis of organic materials by X-ray microscopy.[14] The first step in this effort is an improved understanding of the nature of Rydberg−valence mixing in the simplest situation, for gaseous alkanes.

In the early NEXAFS and inner shell electron energy loss spectroscopy (ISEELS) literature of simple alkanes, the preedge transitions were assigned as Rydberg transitions,[15−17] e.g., carbon 1s → 3s and carbon 1s → 3p transitions. While unresolved, vibronic excitation was used to justify the presence of the dipole forbidden carbon 1s(a_1) → 3s(a_1) transition in methane.[17] Later, and because of comparisons to condensed alkanes, the strong preedge features in the spectra of simple alkanes were assigned as excitations to 3p/π^*(CH_3) mixed Rydberg−valence orbitals, in which the valence orbital has antibonding σ^*(C−H) character.[3,5] With more recent, high-resolution spectra of gaseous alkanes, a clear Rydberg series with vibronic structure is obvious.[1,2,4] High-quality ab initio calculations, such as those by Ueda et al.[1] and Bagus et al.,[12] show that features in the preedge spectra of methane and propane, respectively, are predominantly Rydberg character. Furthermore, resonant Auger spectroscopy measurements of methane by Ueda at al. show a weakly mixed valence component in carbon 1s → Rydberg transitions that have a magnitude as 3s > 3d > 3p.[1] Jahn−Teller effects observed in the methane carbon 1s(a_1) → 3pt_2 Rydberg transition are described by Kosugi as originating from the interaction of the 3pt_2 Rydberg state with the 2t_2* valence states in the distorted molecule.[18] Even though the features in the NEXAFS spectra of methane have strikingly obvious Rydberg character, the role of valence contributions is clearly important. The nature of Rydberg−valence mixing in alkane molecules that are small but nevertheless larger than methane is the focus of this paper.

In this paper, we present the high-resolution carbon 1s NEXAFS spectra of methane, ethane, propane, isobutane, and neopentane and the results of high-quality ab initio calculations on these species. We discuss the vibronic and chemical shift contributions to the distinctive 3s and 3p Rydberg bands in these molecules. The results of ab initio calculations are used to characterize the degree and nature of Rydberg−valence mixing in these spectra and to identify the structural requirements and the symmetry conditions under which significant Rydberg−valence mixing occurs.

2. Experimental Section

Methane (99.97%), ethane (99%), and propane (99.5%) were purchased from Matheson, isobutane (99%) was purchased from Aldrich, and neopentane was purchased from Quality Standards & Research Gases, Inc. (99.9% purity). All gases were used as received.

All near-edge X-ray absorption fine structure (NEXAFS) spectra were recorded using the high-resolution Spherical Grating Monochromator (SGM) of the Canadian Synchrotron Radiation Facility (CSRF) at the Synchrotron Radiation Center of the University of Wisconsin.[19] The entrance and exit slits for these measurements were both 50 μm, corresponding to a resolving power of 2600. The monochromator energy scale was calibrated based on the carbon 1s → 3p($\nu = 0$) transition in CO_2 (g), which was set to the value of 294.96 eV, after Ma et al.[4]

The gas-phase NEXAFS spectra were recorded using the McMaster time-of-flight (TOF) mass spectrometer endstation in total ion yield (TIY) mode. A Ti window (typically 150 nm

* Author to whom correspondence should be addressed. Fax: (306) 966-4730. E-mail: stephen.urquhart@usask.ca.

10.1021/jp045370e CCC: $30.25
Published on Web 02/18/2005

thick) was placed in the beam path in order to suppress higher-order photon contamination from the SGM beamline.

3. Computational Studies

To aid the spectral assignments and to understand the nature of the core excited states, ab initio calculations have been performed using Kosugi's GSCF3 package.[20] Since the electronic relaxation of the core excited states induces significant alterations to the electronic structure, high-level calculations are necessary in order to reliably assign inner shell spectra.[21] These calculations are based on the improved virtual orbital approximation (IVO), which explicitly takes into account the core hole in the Hartree−Fock approximation, and are highly optimized for calculation of core excited states.[22]

The geometries for the isolated molecule calculations (methane through neopentane) were taken from geometry optimization performed using the program GAUSSIAN-98,[23] at the 6/31/* level of theory. GSCF3 calculations were performed using the same basis set as used by Ueda et al. for their high-quality calculations of the carbon 1s NEXAFS spectrum of methane.[1] This basis set consists of primitive basis functions that were taken from (73/7), (73/5), and (6) contracted Gaussian-type functions of Huzinaga et al.[24] for the core excited carbon atom, the other carbon atoms, and hydrogen, respectably. This contraction scheme was (411121/31111/1*/1*) on the core excited carbon atom, (621/41/1*/1*) on the other carbon atoms, and (51/1*) on hydrogen atoms, where the polarization functions were $\zeta_d = 1.335$ and 0.288 for carbon and $\zeta_p = 1.0$ for hydrogen. Additional polarization functions to describe Rydberg transitions were added to the core excited atom: $\zeta_s = 0.075$, 0.0253, 0.01141, 0.00589, 0.00334, 0.00204; $\zeta_p = 0.0440$, 0.0197, 0.01013, 0.00573, 0.00349, 0.00224; $\zeta_d = 0.0282$, 0.01447, 0.00817, 0.00496, 0.00319, 0.00214. Calculations were performed for both singlet and triplet core excited states.

Assignments of the character of each optical orbital are obtained from these calculations. Qualitatively, we expect that spatially compact basis functions will contribute to valence orbitals while spatially diffuse functions will contribute to Rydberg orbitals. We estimate the relative contribution of these basis functions to each type of orbital by considering the square of that basis function's coefficient and report these contributions as a percentage (e.g., normalized by the sum of squares of the coefficients). We only consider basis functions centered on the core excited atom. We have classified the basis functions derived from Huzinaga Gaussian-type functions and the tight d-polarization functions ($\zeta_d = 1.335$ and 0.288) as *valence* and the remaining polarization functions (ζ_s, ζ_p, and ζ_d) as *Rydberg*. The differentiation of Rydberg and valence basis functions is quite subjective, because one might expect the diffuse Huzinaga Gaussian-type functions to have some Rydberg character and perhaps the tighter polarization functions to have some valence character. We acknowledge that this approach is subjective and we intend that it be a guide. We are in no way attempting to determine an absolute "percentage" of Rydberg or valence character to these states but rather to provide a comparative guide to character.

The energies of the vibrational modes in methane, ethane, propane, isobutane, and neopentane are important for the discussion of vibronic effects in the NEXAFS spectra of these molecules. To complement experimental IR values from the literature, we performed a calculation of the energies of vibrational modes for methane, ethane, propane, isobutane, and neopentane, using the B3LYP density functional method at the 6-311+G** level, using the program Spartan '04.[25]

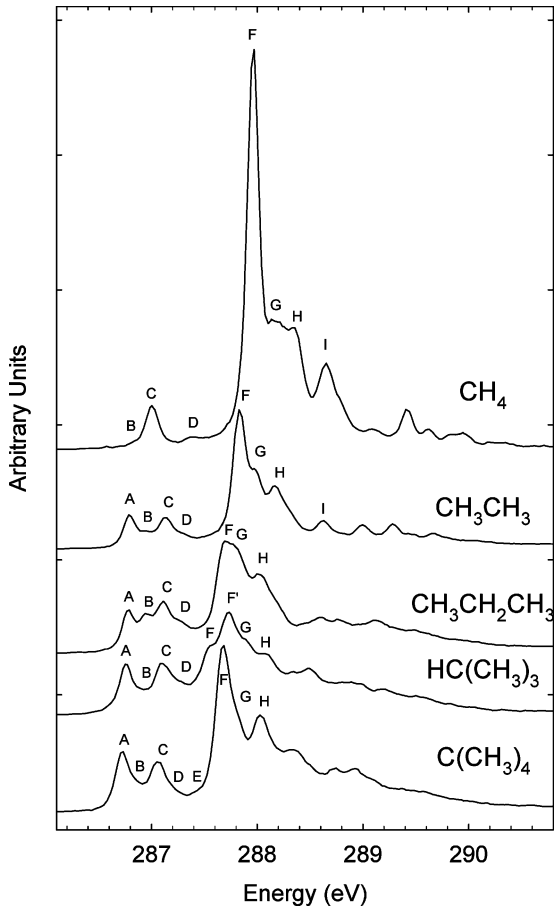

Figure 1. High-resolution carbon 1s near-edge X-ray absorption fine structure (NEXAFS) spectra of gas-phase methane, ethane, propane, isobutane, and neopentane.

4. Results and Discussion

Figure 1 presents the high-resolution carbon 1s NEXAFS gas-phase spectra of methane, ethane, propane, isobutane, and neopentane, recorded using total ion yield (TIY). The energies, term values, and assignments for these spectra are presented in Table 1. The results of high-quality ab initio calculations for these species are presented in Tables 2−6.

The carbon 1s NEXAFS spectra of all five species was previously examined by Hitchcock and Ishii by inner shell electron energy loss spectroscopy with an energy resolution of ~0.6 eV full width at half-maximum.[3] Higher-resolution studies with particularly detailed assignments have been published for methane by Ueda et al.,[1] Kosugi,[18] and Schirmer et al.,[26] for ethane by Y. Ma et al.,[4] and for methane, ethane, and propane by Remmers et al.[2] This is the first time that this complete set of molecules has been studied at a common and relatively high-energy resolution.

Our assignments of methane, ethane, and propane are similar to those of Ueda et al.[1] and Remmers et al.[2] Our assignments for isobutane and neopentane are original. We focus our discussion on the 3s and 3p Rydberg bands that dominate these NEXAFS spectra. While the 3d and higher transitions are clearly resolved in methane,[1] it is difficult to identify these features in larger alkanes where the molecular field lifts the degeneracy of the Rydberg orbitals and significant 3s/3p/3d hybridization occurs.

4.1. Carbon 1s → 3s Band. *4.1.1. Methane*. The carbon $1s(a_1) \rightarrow 3s(a_1)$ transition is dipole forbidden in methane (T_d symmetry). The carbon $1s(a_1) \rightarrow 3s(a_1)$ features observed in

TABLE 1: Experimental Energies, Term Values, and Assignments for the Carbon 1s NEXAFS Spectra of Methane, Ethane, Propane, Isobutane, and Neopentane

		methane		ethane		propane			isobutane			neopentane		
		energy (eV)	assign	Energy (eV)	Assign CH_3	Energy (eV)	Assign. CH_3	Assign CH_2	Energy (eV)	Assign CH_3	Assign CH	Energy (eV)	Assign. CH_3	Assign. C
3s	A	(286.61)[a]	$\nu = 0$	286.79	$\nu = 0$	286.79	$\nu = 0$	-	286.76	$\nu = 0$		286.72	$\nu = 0$	
	B	286.83(3)	$\nu_4 = 1$	286.94(3)	$\nu_2 = 1$	286.95	$\nu_b = 1$	$\nu = 0$	286.95(3)	$\nu_b = 1$		286.85	$\nu_2 = 1$	
	C	287.00	$\nu_3 = 1$	287.14	$\nu_1 = 1$	287.11	$\nu_a = 1$	$\nu_b = 1$	287.11	$\nu_a = 1$	$\nu = 0$	287.07	$\nu_1 = 1$	
	D	287.39(3)	$\nu_3 = 2$	287.31(3)		287.28(3)		$\nu_a = 1$	287.28		$\nu_b = 1$	287.25(3)		
	E											287.45		$\nu(t_2) = 1$
3p	F	287.96	$\nu = 0$	287.83	$\nu = 0$	287.68(3)	$\nu = 0$		287.56	$\nu = 0$		287.68	$\nu = 0$	
	F′								287.73	$\nu = 0$				
	G	288.17(3)	$\nu_4 = 1$	287.98	$\nu_2 = 1$	287.77(3)	$\nu_b = 1$	$\nu = 0$	287.89			287.83	$\nu_2 = 1$	
	H	288.35(3)	$\nu_1 = 1$	288.17	$\nu_1 = 1$	288.02	$\nu_a = 1$	ν_b	288.08			288.03	$\nu_1 = 1$	
3d	I	288.66(3)	3d	288.63	$\nu = 0$									

[a] Hypothetical position of adiabatic transition (see text).

TABLE 2: Calculated Energies, Term Values, Oscillator Strengths, Orbital Size, Single−Triplet Energy Separation, Assignment, and Orbital Contribution from ab Inito Calculations of the Carbon 1s NEXAFS Spectrum of Methane

CH_4 Ionization Potential = 290.892 (eV)

						assignment[c]						
							valance contribution			Rydberg contribution		
	energy (eV)	TV[a] (eV)	oscillator strength[b]	size (Å)	ΔE(S − T) (eV)		s	p	d	s	p	d
	287.269	3.623	0.0000000	3.267	0.222	3s	**12.4%**			**87.6%**		
×3	288.395	2.497	0.0017300[b]	4.204	0.069	3p		5.8%			**92.8%**	**1.4%**
×3	289.219	1.673	0.0012705[b]	4.972	0.027	3d		41.4%	0.3%		**14.7%**	**43.6%**
	289.330	1.562	0.0000000	7.393	0.065	4s	2.3%			**97.7%**		
×2	289.377	1.515	0.0000000[b]	5.931	0.000	3d			0.1%		0.2%	**99.7%**

[a] Term Value = Ionization Potential − Energy. [b] Oscillator strength is given per degenerate transition. [c] Percentage contribution is based on the square of the basis function coefficient to the orbital wave function. Differentiation of valence and Rydberg is subjective; see text.

TABLE 3: Calculated Energies, Term Values, Oscillator Strengths, Orbital Size, Single−Triplet Energy Separation, Assignment, and Orbital Contribution from ab Initio Calculations of the Carbon 1s NEXAFS Spectrum of Ethane

CH_3 Ionization Potential =290.678 (eV)

						assignment[c]						
							valance contribution			Rydberg contribution		
	energy (eV)	TV[a] (eV)	oscillator strength[b]	size (Å)	ΔE(S − T) (eV)		s	p	d	s	p	d
	287.437	3.241	0.0009147	3.727	0.163	3s	**10.6%**	1.2%		**83.2%**	4.6%	0.4%
×2	288.300	2.378	0.0018655[b]	4.476	0.060	3p		8.1%			**86.2%**	5.7%
	288.363	2.315	0.0000110	4.570	0.013	3p +	2.7%	2.3%	0.1%	**21.0%**	**63.0%**	**11.0%**
	289.084	1.594	0.0000403	6.470	0.041	4s/3d	3.5%	0.8%		**78.3%**	4.2%	**13.1%**
×2	289.112	1.566	0.0005658[b]	5.594	0.013	3d		15.0%	0.1%		1.7%	**83.2%**
×2	289.246	1.432	0.0001598[b]	6.506	0.005	3d		0.7%			10.1%	**89.2%**
	289.298	1.380	0.0001954	7.774	0.020	4s/3d	0.1%			**77.9%**	**11.2%**	**10.8%**

[a] Term Value = Ionization Potential − Energy. [b] Oscillator strength is given per degenerate transition. [c] Percentage contribution is based on the square of the basis function coefficient to the orbital wave function. Differentiation of valence and Rydberg is subjective; see text.

the spectrum of methane are dipole allowed because they are accompanied by the excitation of vibrations of t_2 symmetry. There are t_2 symmetry vibrational modes in methane (ν_3 and ν_4) with IR energies of $\upsilon_3 = 0.37$ eV and $\upsilon_4 = 0.16$ eV,[27] respectively (Table 8). The first strong feature in the NEXAFS spectrum of methane at 287.00 eV (Figure 1, peak C) is assigned as the carbon $1s(a_1) \rightarrow 3s$ (a_1; $\upsilon_3 = 1$) transition, and a weak shoulder at slightly lower energy, 286.83 eV (Figure 1, peak B), is assigned as the carbon $1s(a_1) \rightarrow 3s(a_1; \upsilon_4 = 1)$ transition. A third, weaker feature at 287.39 eV (Figure 1, peak D) is assigned as the carbon $1s(a_1) \rightarrow 3s(a_1; \upsilon_3 = 2)$ transition, in agreement with Remmers et al.[2] We can estimate the υ_3 energy as 0.39 eV for the (C $1s^{-1}$; 3s) core excited state in methane and, from this, estimate the energy of the dipole forbidden (adiabatic) carbon $1s(a_1) \rightarrow 3s(a_1; \upsilon = 0)$ transition as 286.61 eV (Figure 1, peak A). The υ_4 vibrational energy for the (C $1s^{-1}$; 3s) core excited state in methane is estimated as 0.22 eV. These (C $1s^{-1}$; 3s) vibrational energies are slightly larger than the IR values ($\upsilon_3 = 0.37$ eV, $\upsilon_4 = 0.16$ eV).[27]

4.1.2. Ethane. In ethane (D_{3D} symmetry), the carbon $1s(a_{1g}) \rightarrow 3s(a_{2u})$ and the carbon $1s(a_{2u}) \rightarrow 3s(a_{1g})$ transitions are dipole allowed, and the adiabatic transition is therefore observed at 286.79 eV (A). Three totally symmetric (a_{1g}) modes can also couple to this dipole allowed transition. While nontotally symmetric vibrational modes undoubtedly couple to the dipole forbidden carbon 1s → 3s transitions ($a_{1g} \rightarrow a_{1g}$; $a_{2u} \rightarrow a_{2u}$), such as those observed above for the 3s band of methane, these transitions will be much weaker than the excitation of totally symmetric vibrational modes coupled to electric dipole allowed transitions. Therefore, we shall neglect vibronic coupling to electronically forbidden transitions in favor of the stronger electronic dipole allowed transitions.

We have so far discussed the symmetry of core excited ethane within the delocalized core hole viewpoint. However, a com-

TABLE 4: Calculated Energies, Term Values, Oscillator Strengths, Orbital Size, Single−Triplet Energy Separation, Assignment, and Orbital Contribution from ab Initio Calculations of the Carbon 1s NEXAFS Spectrum of Propane[d]

CH_3 Ionization Potential = 290.494 (eV)

					assignment[c]						
						valance contribution			Rydberg contribution		
energy (eV)	TV[a] (eV)	oscillator strength[b]	size (Å)	ΔE(S − T) (eV)		s	p	d	s	p	d
287.427	3.067	0.0010901	4.157	0.152	3s	7.5%	1.1%		**84.8%**	5.4%	1.2%
288.187	2.307	0.0015933	4.715	0.051	3p		5.4%			**86.5%**	8.1%
288.194	2.300	0.0014989	4.761	0.049	3p	0.2%	8.0%		2.0%	**84.1%**	5.7%
288.397	2.097	0.0003715	5.024	0.015	3p +	0.8%	3.6%		**19.4%**	**59.3%**	**16.9%**
288.935	1.559	0.0004082	6.256	0.024	4s/4d	1.5%	5.2%		**61.0%**	4.4%	**27.9%**
289.026	1.468	0.0001741	6.607	0.014	4s/3d	0.3%	3.1%		**48.4%**	1.0%	**47.2%**
289.026	1.468	0.0005679	6.223	0.014	3d		16.5%			4.0%	**79.5%**
289.072	1.422	0.0002827	6.596	0.010	3d/3p	0.1%	1.6%		3.7%	19.3%	**75.3%**
289.093	1.401	0.0000377	6.715	0.002	3d		0.8%			12.1%	**87.1%**
289.137	1.357	0.0002042	8.114	0.025	4s +	1.5%	0.2%		72.0%	14.3%	**12.0%**

CH_2 Ionization Potential = 290.543 (eV)

					assignment[c]						
						valance contribution			Rydberg contribution		
energy (eV)	TV[a] (eV)	oscillator strength[b]	size (Å)	ΔE(S − T) (eV)		s	p	d	s	p	d
287.617	2.926	0.0015433	4.025	0.11	3s	8.0%	2.4%		**80.5%**	8.3%	0.8%
288.25	2.293	0.0019389	4.592	0.052	3p		14.2%			**85.2%**	0.6%
288.358	2.185	0.0000457	4.866	0.019	3p +	2.5%	0.4%		**34.5%**	**47.9%**	**14.6%**
288.453	2.090	0.0001099	5.199	0.003	3p		2.2%			**84.4%**	12.4%
288.968	1.575	0.0001198	6.092	0.029	4s/3d	2.7%	4.7%		**45.1%**	0.3%	**47.1%**
289.096	1.447	0.0004979	6.357	0.015	3d/3p		11.0%			18.7%	70.3%
289.114	1.429	0.0000161	6.699	0.010	3d +	3.2%	2.2%		**24.0%**	**11.5%**	**59.1%**
289.119	1.424	0.0000769	6.580	0.005	3d/3p		0.6%			**10.9%**	**88.5%**
289.145	1.397	0.0000000	6.726	0.000	3d					**100%**	
289.234	1.309	0.0003009	8.339	0.014	4s +	0.6%	0.1%		**83.8%**	4.5%	**11.0%**

[a] Term Value = Ionization Potential − Energy. [b] Oscillator strength is given per degenerate transition. [c] Percentage contribution is based on the square of the basis function coefficient to the orbital wave function. Differentiation of valence and Rydberg is subjective; see text. [d] Propane is oriented with the C_2 axis along the z axis and C−C−C in the yz plane; isobutane is oriented with the C_3 axis along z.

bined theoretical and experimental analysis of the vibrational fine structure observed in the carbon 1s X-ray photoelectron spectrum of ethane indicates that a localized core hole description is appropriate.[28]

From the IR spectroscopy of ethane,[27] the vibrational energies of the totally symmetric υ_1, υ_2, and υ_3 modes (a_{1g} symmetry in the D_{3d} point group) are 0.36, 0.17, and 0.12 eV and are assigned as the C−H stretch, C−H deformation, and the C−C stretch, respectively. When a localized carbon 1s core hole is created, the molecular symmetry will be reduced to the C_{3v} point group, and there are now five totally symmetric (a_1) vibrational modes. Two modes are derived from υ_1, and two modes are derived from υ_2, but the C−C stretch (υ_3) is not affected by the descent in symmetry. The doubling of the υ_1 and υ_2 transitions will not necessarily lead to more vibrational features. As an approximation, we can consider only vibrational modes that have a displacement in bonds to the core excited carbon atom.[29] In the X-ray photoelectron spectroscopy (XPS) spectrum of ethane, the two C−H stretch modes (derived from υ_1 in D_{3d} symmetry) are strongly localized to each carbon atom, one on the core excited atom and the other on the un-ionized atom, and the two C−H deformation modes (derived from υ_1 in D_{3d} symmetry) are only partially localized.[28] Therefore, only one C−H stretch mode will contribute to the spectrum, but contributions are expected from each C−H deformation mode. In the high-resolution carbon 1s XPS spectra of ethane, no excitation of the C−C stretching mode is observed.[28] Even so, we do not expect to resolve the υ_2 (C−H deformation) and υ_3 (C−C stretch) vibrational bands as these are only slightly different in energy. A comparison of the high-resolution carbon 1s NEXAFS spectra of ethane and deuterated ethane[2,4] shows strong shifts in the vibronic structure with deuteration. If this normal mode was dominated by a C−C stretch, then only a very modest effect would be observed with deuteration. We therefore assign the second feature at 286.94 eV (Figure 1, peak B) as the carbon 1s → 3s ($\upsilon_2 = 1$) transition, where υ_2 is the label of the C−H deformation. The third feature at 287.14 eV (Figure 1, peak C) is assigned as the C 1s → 3s($\upsilon_1 = 1$) transition.

The intensities of the vibrational bands, with the strongest transition for $\upsilon = 0$ and progressively weaker transitions for higher values of υ, are consistent with the interpretation of predominantly Rydberg character for these core excited states. In contrast, a highly antibonding core excited state, such as the (N $1s^{-1}$; π^*) state of N_2, would lead to a different Franck−Condon profile where the adiabatic transition would not be the most intense. Superficially, the Franck−Condon profile in the NEXAFS spectrum of ethane is similar to that observed in the XPS spectrum of ethane, where analysis indicates a small decrease in the C−H bond length with the creation of the core hole.[28] However, in core excitation, we must consider the effect of the electron in the optical orbital on the molecule's bonding. If a particular excited state had some valence/antibonding character, then this antibonding character would lead to an increase in bond length and a decrease in the energy of the stretching vibrational modes. The XPS spectrum of ethane shows an energy of 404.9 meV for the υ_1 mode[28] while our NEXAFS spectrum shows a value of 345 meV for this mode, slightly smaller than the ground state (IR) energy of 361 meV. This implies some C−H antibonding character to this 3s excited state, which would weaken the C−H bond relative to the ground state and overcome the bond shortening expected from photoionization. Similar effects are observed for the 3s Rydberg transitions

TABLE 5: Calculated Energies, Term Values, Oscillator Strengths, Orbital Size, Single−Triplet Energy Separation, Assignment, and Orbital Contribution from ab Initio Calculations of the Carbon 1s NEXAFS Spectrum of Isobutane

CH_3 Ionization Potential = 290.349 (eV)

						assignment[c]						
							valance contribution			Rydberg contribution		
	energy (eV)	TV[a] (eV)	oscillator strength[b]	size (Å)	ΔE(S − T) (eV)		s	p	d	s	p	d
	287.413	2.936	0.0011938	4.413	0.142	3s	5.2%	0.9%		**85.7%**	7.0%	1.1%
	288.099	2.250	0.0013142	4.865	0.042	3p	0.1%	4.8%		1.0%	**88.7%**	5.4%
	288.219	2.130	0.0016360	5.190	0.050	3p		9.9%			**85.2%**	4.9%
	288.400	1.949	0.0001430	5.438	0.007	3p +	0.4%	1.0%		**39.4%**	**50.2%**	9.0%
	288.859	1.490	0.0005369	6.608	0.024	4s/3d	0.4%	3.7%		**71.1%**	4.9%	**20.0%**
	288.915	1.434	0.0004769	6.484	0.010	3d/3p		14.1%	0.1%		13.8%	**72.1%**
	288.932	1.417	0.0002666	6.722	0.012	3d +	0.1%	3.2%		**39.4%**	7.5%	**49.8%**
	288.964	1.385	0.0002215	6.888	0.005	3d/3p		0.3%			26.5%	**73.2%**
	288.967	1.382	0.0000311	6.886	0.003	3d +	0.1%	1.5%		**16.1%**	8.0%	**74.3%**
	289.004	1.345	0.0002592	8.404	0.031	4s +	1.7%	0.2%		**74.3%**	**16.2%**	7.6%

CH Ionization Potential = 290.467 (eV)

						assignment[c]						
							valance contribution			Rydberg contribution		
	energy (eV)	TV[a] (eV)	oscillator strength[b]	size (Å)	ΔE(S − T) (eV)		s	p	d	s	p	d
	287.809	2.658	0.0016136	4.352	0.060	3s/3p	3.9%	4.1%		**80.7%**	**10.4%**	0.8%
	288.335	2.132	0.0003702	5.034	0.025	3s/3p	1.7%	4.2%		**47.7%**	**46.1%**	0.4%
×2	288.495	1.972[b]	0.0000795[b]	5.533	0.003	3p		1.2%		**88.1%**	**10.7%**	
	289.002	1.465	0.0002651	6.564	0.028	4s/3d	5.1%	1.6%		**44.6%**	8.6%	**40.1%**
×2	289.053	1.414[b]	0.0000859	6.602	0.004	3d		1.2%		3.3%	**95.5%**	
×2	289.087	1.380[b]	0.0000275	6.844	0.000	3d		2.0%		3.3%	**94.7%**	
	289.215	1.252	0.0003136	8.880	0.010	4s	0.7%	0.2%		**88.6%**	5.5%	5.0%

[a] Term Value = Ionization Potential − Energy. [b] Oscillator strength is given per degenerate transition. [c] Percentage contribution is based on the square of the basis function coefficient to the orbital wave function. Differentiation of valence and Rydberg is subjective; see text.

TABLE 6: Calculated Energies, Term Values, Oscillator Strengths, Orbital Size, Singlet−Triplet Energy Separation, Assignment, and Orbital Contribution from ab Initio Calculations of the Carbon 1s NEXAFS Spectrum of Neopentane

CH_3 Ionization Potential = 290.346 (eV)

						assignment[c]						
							valance contribution			Rydberg contribution		
	energy (eV)	TV[a] (eV)	oscillator strength[b]	size (Å)	ΔE(S − T) (eV)		s	p	d	s	p	d
	287.510	2.836	0.0012499	4.588	0.135	3s	5.1%	0.9%		**85.0%**	8.1%	0.9%
×2	288.290	2.056	0.0013981[b]	5.375	0.045	3p		8.0%			**86.2%**	5.8%
	288.487	1.859	0.0000047	5.756	0.003	4s/3p		0.1%		**56.7%**	**41.8%**	1.3%
	288.927	1.419	0.0002254	6.882	0.013	4s +		0.8%		**70.4%**	**11.2%**	**17.5%**
×2	288.937	1.409	0.0005917[b]	6.711	0.014	3d/3p		10.7%			**23.8%**	**65.4%**
×2	288.989	1.357	0.0000946[b]	7.061	0.003	3d/3p		0.5%			**20.0%**	**79.5%**
	289.009	1.337	0.0003397	8.696	0.043	4s/3p	2.0%	0.1%		**81.5%**	**13.9%**	2.5%

C Ionization Potential = 290.530 (eV)

						assignment[c]						
							valance contribution			Rydberg contribution		
	energy (eV)	TV[a] (eV)	oscillator strength[b]	size (Å)	ΔE(S − T) (eV)		s	p	d	s	p	d
	288.147	2.383	0.0000000	4.967	0.003	3s	0.1%			**99.9%**		
×3	288.642	1.888	0.0000583[b]	5.800	0.005	3p		0.3%			**98.0%**	1.7%
×3	289.129	1.401	0.0001272[b]	6.680	0.004	3d		0.5%			4.8%	**94.6%**
×2	289.174	1.356	0.0000000[b]	6.994	0.001	3d					**100%**	
	289.347	1.183	0.0000000	9.659	0.000	4s	0.2%			**99.8%**		

[a] Term Value = Ionization Potential − Energy. [b] Oscillator strength is given per degenerate transition. [c] Percentage contribution is based on the square of the basis function coefficient to the orbital wave function. Differentiation of valence and Rydberg is subjective; see text.

of propane, isobutane, and neopentane and the 3p Rydberg transitions in ethane.

4.1.3. Propane and Isobutane. The carbon 1s NEXAFS spectra of propane and isobutane will be complex, because these molecules have two chemically inequivalent carbon atoms and the relatively lower symmetry will lead to nine totally symmetric vibratonal modes in propane (ground state C_{2v} symmetry) and eight totally symmetric vibrational modes in isobutane (ground state C_{3v} symmetry).

We can estimate the magnitude of the shift between the two chemically inequivalent carbon atoms from our ab initio calculations (Tables 2−6). These calculations predict that the energy of the carbon 1s → 3s(v = 0) transition will shift by +0.190 eV between the CH_3 and the CH_2 group in propane

TABLE 7: Summary of Singlet−Triplet Energy Differences and Orbital Size for Carbon 1s → 3s and 3p Transitions in Methane, Ethane, Propane, Isobutane, and Neopentane

		3s S−T (eV)	size (Å)	3p S−T (eV)	size (Å)	3p character
CH_4	methane	0.222	3.267	0.069 (3x)	4.204	C−H
CH_3	ethane	0.163	3.727	0.060 (2x)	4.476	C−H
				0.013	4.570	C−C
	propane	0.152	4.157	0.051	4.715	C−H
				0.049	4.761	C−H
				0.015	5.024	C−C
	isobutane	0.142	4.413	0.042	4.865	C−H
				0.050	5.190	C−H
				0.007	5.438	C−C
	neopentane	0.135	4.588	0.045 (×2)	5.375	C−H
				0.003	5.756	C−C
CH_2	propane	0.110	4.025	0.052	4.592	C−H
				0.019	4.866	C−C
				0.003	5.199	C−C
CH	isobutane	0.060	4.352	0.025	5.034	C−H
				0.003 (×2)	5.533	C−C
C	neopentane	0.003	4.967	0.005 (×3)	5.800	C−C

and by +0.396 eV between the CH_3 and the CH group in isobutane. This shift is demonstrated in Figure 2, which presents a line spectrum based on the ab initio calculations (circle, CH_4; square, CH_3; triangle, CH_x for 3s and 3p transitions). As the energy of the vibrational modes ranges between 0.05 and 0.36 eV, we expect significant overlap between vibrational excitation and chemical shifts in propane but less overlap in isobutane.

The calculated and experimental (IR) vibrational mode energies are presented in Table 8. While there are many totally symmetric vibrational modes in these molecules, we can group these modes into two bands as the energy separation between most modes is less than the core hole lifetime broadening. The first band consists of the three most energetic vibrational modes (C−H stretches, υ_1, υ_2, and υ_3), with an energy around ∼0.375 eV. For simplicity, we will refer to this as the υ_a band. The vibrational energies for the second band (υ_4, υ_5, υ_6, etc.) range from 0.18 to 0.05 eV, a separation that would be difficult to resolve. The band formed from these unresolved vibrations is referred to as the υ_b band. We will use the υ_b and υ_b labeling for propane and isobutane only and the conventional numbering scheme for the higher-symmetry alkane molecules.

The first transition in the spectra of propane and isobutane is assigned as the dipole allowed carbon 1s(CH_3) → 3s($\upsilon = 0$) transition (Figure 1, peak A). The broad second peak in propane (Figure 1, peak B) is assigned as an overlap of the chemically shifted carbon 1s (CH_2) → 3s($\upsilon = 0$) transition and the carbon 1s(CH_3) → 3s($\upsilon_b = 1$) bands. Here, $\upsilon_b = 1$ is meant to imply excitation of one of the overlapping lower-energy vibrational modes (e.g., υ_4, υ_5, υ_6, etc.). From the ab initio calculations, we expect the carbon 1s(CH_2) → 3s($\upsilon = 0$) transition in ethane to occur 0.19 eV above the carbon 1s(CH_3) → 3s($\upsilon = 0$) transition (Figure 2). This second peak (Figure 1, peak B) in propane is quite broad as expected for an overlap of several features. The third band (287.11 eV, Figure 1, peak C) is assigned as an overlap of the carbon 1s(CH_3) → 3s($\upsilon_a = 1$) and carbon 1s(CH_2) → 3s($\upsilon_b = 1$) transitions. The fourth band (287.31 eV, Figure 1, peak D) is tentatively assigned as the carbon 1s(CH_2) → 3s($\upsilon_a = 1$) transition.

In isobutane, the chemical shift between the CH_3 group and the CH group is larger, predicted by calculations to be +0.396 eV (Figure 2). Therefore, the second transition in this spectrum (Figure 1, peak B) is assigned as the carbon 1s(CH_3) → 3s($\upsilon_b = 1$) band, as the carbon 1s(CH_2) → 3s($\upsilon = 0$) transition is shifted to a higher energy. The second feature is weaker in isobutane than in propane because of this shift. The third feature in isobutane, at 287.11 eV (Figure 1, peak C), is assigned as an overlap of the carbon 1s(CH_3) → 3s($\upsilon_a = 1$) and carbon 1s(CH_2) → 3s($\upsilon = 0$) transitions. The fourth feature (287.28 eV, Figure 1, peak D) is tentatively assigned as the carbon 1s(CH_2) → 3s($\upsilon_b = 1$) transition.

4.1.4. Neopentane. Neopentane has a much simpler NEXAFS spectrum than that isobutane or propane. As neopentane has high (T_d) symmetry, there are only three totally symmetric vibrations with the following IR energies: $\upsilon_1 = 0.375$ eV, $\upsilon_2 = 0.178$ eV, $\upsilon_3 = 0.090$ eV.[30] The NEXAFS spectrum of neopentane is superficially similar to ethane, which is expected as neopentane is dominated by the CH_3 group contribution. The first peak in the carbon 1s NEXAFS spectrum of neopentane (Figure 1, peak A) is assigned as the dipole allowed carbon 1s(CH_3) → 3s($\upsilon = 0$) transition. A weak shoulder at 286.85 eV (Figure 1, peak B) is assigned as the carbon 1s(CH_3) → 3s($\upsilon_2 = 1$) transition, and the strong feature at 287.07 eV (Figure 1, peak C) is assigned as the carbon 1s(CH_3) → 3s($\upsilon_1 = 1$) transition. We can calculate the υ_1 vibrational energy for core excited neopentane as ∼0.34 eV, which is slightly smaller than the IR energy of 0.361 eV.

Can we resolve the carbon 1s(C) → 3s($\nu = 0$) transition in neopentane? There are several reasons why this feature will be extremely weak. Our ab initio calculations (Table 6) predict that the carbon carbon 1s → 3s transition energy for the central carbon will occur +0.637 eV higher than the methyl group carbon 1s → 3s transition energy (Figure 2). This should place this transition just below the strong 3p Rydberg manifold for the CH_3 groups. Second, the carbon 1s → 3s transition for the central carbon atom will be dipole forbidden, as this transition is $a_1 \rightarrow a_1$ in the T_d point group of neopentane. Therefore, this transition must couple to vibrations of appropriate (t_2) symmetry to occur. In neopentane, there are 21 t_2 normal modes (seven sets of 3-fold degenerate normal modes), with only the lower-energy modes showing significant C−C atomic displacement involving the central carbon atom. Finally, this feature should be weak because there is only one central carbon and a background from the four CH_3 groups. Where would this feature appear? The calculated chemical shift for the carbon 1s → 3s transition, between the CH_3 group and the central carbon atom, is 0.637 eV. This would place this feature around 287.36 eV, plus some additional energy for the required t_2 vibrational normal mode. We tentatively assign the weak shoulder at 287.45 eV (Figure 1, peak E) as this central carbon carbon 1s → 3s ($\upsilon_{t_2} = 1$) transition.

4.2. 3p Band: Experimental Observations. *4.2.1. Methane.* The carbon 1s → 3p($\upsilon = 0$) (Figure 1, peak F) transition in methane is extremely intense, relative to the other molecules in this series. In methane, the 3p Rydberg orbitals are degenerate, while in the other species the molecular field lifts the degeneracy and the 3p Rydberg transition is broader.

The shoulder immediately above the intense carbon 1s → 3p($\upsilon = 0$) transition may originate from some degree of Jahn−Teller distortion. Tronc et al.[31] and Wight et al.[32] have assigned the 288.66 eV feature (Figure 1, peak I) as originating from Jahn−Teller splitting of the carbon 1s → 3p transition, although Ueda et al.[1] have shown that this 288.66 eV feature is a carbon 1s → 3d transition. Kosugi[18,33] has argued that an atomic-like (pure) 3p Rydberg state should only have a very small Jahn−Teller distortion but that the presence of strong nontotally symmetric vibrational contributions (Figure 1, peak G) to the

TABLE 8: Energies for the Totally Symmetric Vibrational Modes for Methane, Ethane, Propane, Isobutane, and Neopentane

methane (T_d)[a]			ethane (D_{3D})			propane (C_{2V})			isobutane (C_{3v})			neopentane (T_d)			
	calcd	expt[27]		calcd	expt[27]		calcd	expt[34]		calcd	expt[35]		calcd	expt[30]	
υ_3 (t_2)	0.388	0.374													
υ_1 (a_1)	0.375	0.361	υ_1	0.375	0.359	υ_1	0.382	0.369	υ_1	0.382	0.368	υ_1	0.375	0.361	C−H
						υ_2	0.374	0.367	υ_2	0.374	0.360				
						υ_3	0.373	0.358	υ_3	0.371	0.360				
						υ_4	0.187	0.183							
						υ_5	0.184	0.181	υ_4	0.188	0.182				
υ_4 (t_2)	0.167	0.162	υ_2	0.176	0.170	υ_6	0.176	0.173	υ_5	0.177	0.172	υ_2	0.178	-	
						υ_7	0.146	0.144	υ_6	0.150	0.147				
			υ_3	0.123	0.123	υ_8	0.108	0.108	υ_7	0.100	0.099	υ_3	0.090	0.091	
						υ_9	0.046	0.046	υ_8	0.053	0.054				

[a] Energies for the t_2 modes, which couple to the dipole forbidden C 1s(a_1) → 3s(a_1) transition, are included for methane.

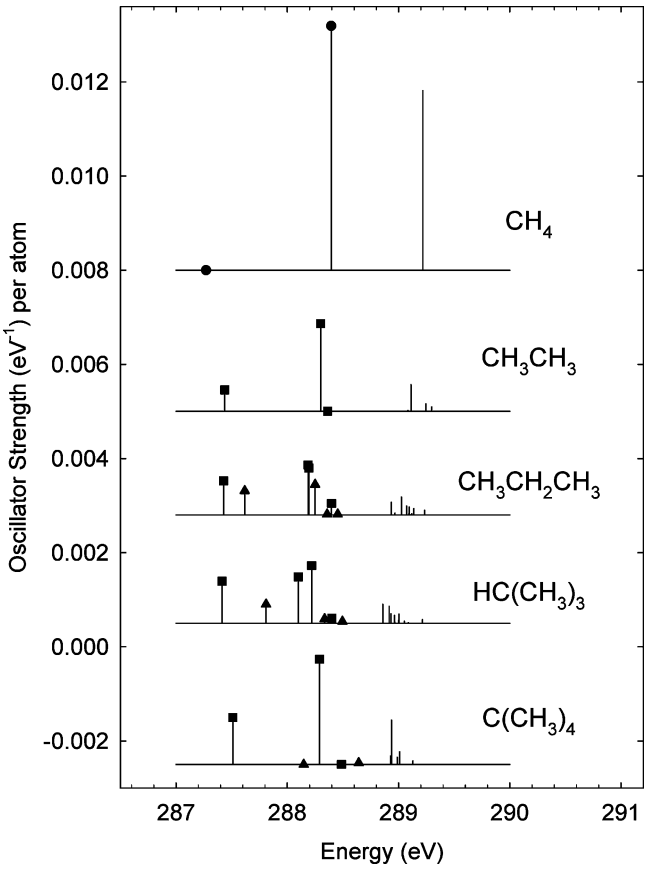

Figure 2. Representation of the 3s, 3p, and 3d/4s Rydberg components in the carbon 1s near-edge X-ray absorption fine structure (NEXAFS) spectra of gas-phase methane, ethane, propane, isobutane, and neopentane, as calculated by ab initio improved virtual orbital calculations. The energy and oscillator strength for each transition is show as a line. Lines that appear below 288 eV arise from carbon 1s → 3s transitions; the lines between 288 and 288.8 eV arise from carbon 1s → 3p transitions, and those above 288.8 eV are due to carbon 1s → 3d or carbon 1s → 4s transitions. A symbol represents the type of carbon atom: circle, CH_4; square, CH_3 group; triangle, CH_2, CH, or C atom. The lines without symbols are from carbon 1s → 3d or carbon 1s → 4s transitions (Tables 2−6). The intensities are weighted by the molecular stoichiometry and are divided by the total number of carbon atoms in each molecule.

3p Rydberg indicates a substantial interaction between a C_{3v} distorted 3p(t_2) Rydberg excited state and a carbon 1s(a_1) → $2t_2$* valence excited state.

Our assignments for the 3p band of methane are based on those of Kosugi.[18,33] The first shoulder in this band, at 288.17 eV (Figure 1, peak G), is assigned as the excitation of nontotally symmetric vibrational modes. Kosugi resolves several components in this shoulder.[33] The second shoulder at 288.35 eV (Figure 1, peak H) is assigned as a vibronic excitation to the totally symmetric υ_1 vibrational mode. The sharp feature at 288.66 eV (Figure 1, peak I) is assigned as the carbon 1s → 3d transition, in agreement with Ueda et al.[1]

4.2.2. Ethane. The C 1s → 3p($\upsilon = 0$) transition in ethane should be split into several components because of the reduction of symmetry relative to methane. In Figure 2 and Table 3, we see that doubly degenerate components of the carbon 1s → 3p($\upsilon = 0$) transition shift to lower energy and that the third component is vanishingly small. The weak component is along the C−C bond, while the two strong components are perpendicular to the C−C bond (e.g., C−H character) and have some 3s and 3d character, more than that in methane. This "weak" 3p feature and the reduced symmetry decrease the overall intensity of the carbon 1s → 3p($\upsilon = 0$) transition relative to methane. The two vibrational features above the carbon 1s → 3p($\upsilon = 0$) transition, at 287.98 eV (Figure 1, peak G) and 288.17 eV (Figure 1, peak H), are assigned as the carbon 1s → 3p($\upsilon_2 = 1$) and carbon 1s → 3p($\upsilon_1 = 1$) transitions, respectively. The υ_1 energy is similar to that observed for the (C $1s^{-1}$; 3s) state in ethane.

4.2.3. Propane and Isobutane. The 3p bands in propane and isobutane are more complicated as chemical shifts, the nondegeneracy of the 3p Rydberg orbitals, and vibrational features all play significant roles. In Figure 2, Table 4, and Table 5, we can see that the 3p Rydberg orbitals are split into three components in propane and isobutane.

For the CH_3 group contribution in propane and isobutane, the 3p component directed along the C−C bond is the weakest, and the two 3p components perpendicular to the C−C bond (e.g., stronger C−H character) are much stronger. For the CH_2 group of propane, we find that the 3p component directed along the C−H bonds is the strongest (*x* axis) and the two components in the C−C−C plane (*yz*) are weaker. For the C−H group of isobutane, the component directed along the single C−H bond is stronger than those directed normal to this bond. By symmetry, only 3p Rydberg orbitals directed along the C−H bond can mix with σ*(C−H) valence states. Transitions to 3p Rydberg orbitals that share the same directionality as the C−H bond are more intense, although the intensity of the "C−H" carbon 1s → 3p transition in isobutane is weaker than that in other molecules.

In the NEXAFS spectrum of propane, the 3p peak is broader than that in ethane or methane. The ab initio calculations predict that the CH_3 group has two strong carbon 1s → 3p transitions with an energy separation of only 0.007 eV but that the CH_2 group has a carbon 1s → 3p transition 0.093 eV higher in energy than the lowest-energy carbon 1s(CH_3) → 3p transitions. The 287.77 eV shoulder (Figure 1, peak G) above the main carbon

1s(CH_3) → 3p($v = 0$) transition (Figure 1, peak F) is therefore assigned as the carbon 1s(CH_2) → 3p($v = 0$) transition, and the well-resolved feature at 288.02 eV (Figure 1, peak H) is assigned as the carbon 1s(CH_3) → 3p($v_1 = 1$) transition.

The 3p band in isobutane is very curious. A lower-energy shoulder (287.56 eV, Figure 1, peak F) only appears in the spectrum of isobutane. From our ab initio calculations (Figure 2 and Table 5), we see that the C 1s(CH_3) → 3p Rydberg transition is split into three components and that the lowest-energy component is lower than any other 3p feature in this series. We assign the 287.56 eV shoulder (Figure 1, peak F) as a carbon 1s(CH_3) → 3p($v = 0$) transition associated with this 3p Rydberg, as split by the molecular field. The second feature at 287.73 eV (Figure 1, peak F′) contains contributions from the intermediate 3p Rydberg transition as well as vibronic features associated with the lower-energy 3p Rydberg transition.

Above these features, the spectrum is quite subtle, as there are chemical shifts due to the molecular field and the chemical differences between the CH_3 and CH sites (Table 5) as well as a wide manifold of vibronic features for the CH_3 and CH sites.

4.2.4. Neopentane. The 3p band in neopentane is quite simple and similar to ethane. There are only three totally symmetric vibrations in neopentane, and the chemical shift between carbon 1s → 3p($v = 0$) transition for the CH_3 and the central carbon is predicted to be +0.352 eV by ab initio calculations. A weak shoulder is observed at 287.83 eV (Figure 1, peak G), and a well-resolved feature is observed at 288.03 eV (Figure 1, peak H). The second feature is assigned as the carbon 1s → 3p($v_2 = 1$) transition, which gives a v_2 vibratonal energy of 0.15 eV, slightly less than the IR value of the v_2 mode (0.178 eV). The strong feature at 288.03 eV (Figure 1, peak H) is assigned as the carbon 1s → 3p($v_1 = 1$) transition.

5. Rydberg−Valence Mixing: Insights from ab Initio Calculations

As shown above, high-quality ab initio calculations are useful for interpreting molecular NEXAFS spectra. Here, we use these calculations to examine the nature of Rydberg−valence mixing. The degree of Rydberg−valence mixing can be revealed by considering the difference between calculated singlet and triplet excitation energies for a transition, the contribution of Rydberg and valence basis functions, and the size of the optical orbital.

If a core electron is excited to a pure Rydberg orbital, then its interaction with other valence electrons will be extremely small. In contrast, if the core electron is excited to a valence orbital, then there will be a much stronger interaction with the other valence electrons. By the Pauli exclusion principle, the excited electron will have less repulsion with the other electrons if it is in a triplet excited state than in a singlet excited state. Therefore, a greater difference in the singlet−triplet excitation energies is expected if the optical orbital has a larger valence character. As an approximate guide, a singlet−triplet energy difference greater than 0.05 eV implies some valence character.

Table 7 presents a summary of singlet−triplet energy differences and orbital sizes for the carbon 1s → 3s and the carbon 1s → 3p transitions. From the larger single−triplet energy differences, we can see that the valence character is greater for the 3s states relative to the 3p states. This result is consistent with the interpretation of the participant Auger spectra of methane of Ueda at al.[1] For the carbon 1s → 3s transitions, the degree of valence character scales with the number of hydrogen atoms directly bonded to the core excited atom. If we examine the series CH_4, CH_3, CH_2, CH, C, e.g., from methane to the central atom of neopentane, we observe a clear decrease in the valence character as the number of C−H bonds decreases. In particular, the carbon 1s → 3s transition for the central atom in neopentane, which has no C−H bonds, is entirely Rydberg character. This observation illustrates a key point; there can only be Rydberg valence mixing when there is a valence orbital of appropriate symmetry and energy. Here, this would be a C−H valence orbital (e.g., σ^*(C−H)). If we examine the core → 3s transitions for the methyl groups (e.g., ethane to neopentane), then we also see that the valence character decreases in this series of molecules but not to the same extent as when C−H bonds are added or removed. In addition, the oscillator strength of this core → 3s transition increases as its valence character decreases.

If we examine the basis functions that contribute to the calculated carbon 1s → 3s transitions (Tables 2−6), we observe that the role of "valence" 3s polarization functions decreases for the CH_4, CH_3, CH_2, CH, C series as the Rydberg 3p increases. An exception to this trend is the carbon 1s → 3s transition in neopentane, which is forbidden and expected to be entirely Rydberg due to the absence of C−H valence contributions.

The trend in the character of the carbon 1s → 3s transition for the CH_3 group in the series ethane, propane, isobutane, and neopentane is subtle, a slight decrease in valence character can be inferred from the decrease in the singlet−triplet energy difference (summarized in Table 7). This decrease is smaller than for the series CH_4, CH_3, CH_2, CH, C and cannot be attributed to the number of C−H bonds to the core excited carbon atom. It is evident, from the basis function contributions to the 3s orbitals (Tables 3−6), that the decrease in valence character from the singlet−triplet energy difference can be related to a decrease in valence s symmetry basis functions and an increase in 3p Rydberg symmetry basis functions. Increased 3s−3p hybridization appears to be responsible for this increased Rydberg character from methane (CH_4) to the lower symmetry molecules.

The situation for the carbon 1s → 3p transitions is more complex. The singlet−triplet energy differences are smaller for these 3p transitions than for the 3s transitions. This is expected as the p-symmetry of the Rydberg orbital will have a smaller overlap with the core and other valence electrons, and therefore the repulsion from the Pauli exclusion principle will be reduced. We see a decrease in valence character from methane to neopentane, for the central carbon and for the CH_3 groups, mirroring the character of the carbon 1s → 3s transitions. We also note that the valence character is increased for 3p Rydberg transitions aligned along C−H bonds. Valence character is nearly nonexistent for 3p Rydberg transitions aligned along C−C bonds. This demonstrates that Rydberg−valence mixing can only occur when there is a symmetry allowed overlap between σ^*(C−H) transitions and the 3p Rydberg orbitals.

An evaluation of the orbital contributions for the carbon 1s → 3p transitions shows that strong transitions (generally with higher valence C−H character) are dominated by 3p Rydberg basis functions but with significant p-valence (5−8%) and 3d Rydberg (5−8%) character. The weaker carbon 1s → 3p transitions (generally with higher Rydberg character) are exemplified by mixed 3s/3p/3d hybridization. An evaluation of the size of the orbitals closely follows the trend in the Rydberg−valence character from the singlet−triplet energy differences: the greater the Rydberg character, the greater the size of the orbital.

We have not considered the carbon 1s → 3d Rydberg transitions in much detail. Carbon 1s → 3d transitions can only be clearly resolved in methane, where a strong transition is observed at 288.66 eV (Figure 1, peak I). From the ab initio calculations for this transition (Table 2 and ref 33), 3d Rydberg/p-valence hybridization is observed. In ethane, the strongest carbon 1s → 3d transition has a significant p-valence contribution. In propane, the degeneracy of the 3d transitions is lifted, and the calculations predict many weak transitions with a slight energy separation. Of these, the stronger transitions have significant p-valence−3d hybridization, while the weaker transitions show 3s−3d hybridization. A similar situation is observed for neopentane, except that fewer separate carbon 1s → 3d lines are present in this higher-symmetry molecule.

Conclusions

We have examined the high-resolution carbon 1s NEXAFS spectra of gaseous methane, ethane, propane, isobutane, and neopentane. We have proposed new assignments for the spectra of isobutane and neopentane and evaluated the role of vibronic excitation, the nature of chemical shifts between chemically inequivalent carbon atoms, and the effect of the molecular field on the spectra of these molecules. Our ab initio calculations show that Rydberg−valence mixing is present when there are excited states of valence σ^*(C−H) character that have the appropriate symmetry to mix with excited states of Rydberg character. Specifically, this degree of valence character scales with the number of C−H bonds to the core excited carbon atom.

Acknowledgment. Research was carried out using the Spherical Grating Monochromator of the Canadian Synchrotron Radiation Facility (CSRF) at the Synchrotron Radiation Center (SRC) of the University of Wisconsin−Madison. The SRC is supported by the National Science Foundation under award number DMR-0084402. The CSRF is supported by the National Science and Engineering Research Council (NSERC) Major Facilities Access Grant. This research was supported by NSERC, the University of Saskatchewan (S.G.U.), and the Nixon Fund (R.G.). The authors are grateful to A. Hitchcock for help with the operation of the McMaster TOF spectrometer and to the staffs of the SRC and CSRF, particularly Y. F. Hu.

References and Notes

(1) Ueda, K.; Okunishi, M.; Chiba, H.; Shimizu, Y.; Ohmori, K.; Sato, Y.; Shigemasa, E.; Kosugi, N. *Chem. Phys. Lett.* **1995**, *236*, 311.

(2) Remmers, G.; Domke, M.; Kaindl, G. *Phys. Rev. A* **1993**, *47*, 3085.

(3) Hitchcock, A. P.; Ishi, I. *J. Electron Spectrosc. Relat. Phenom.* **1987**, *42*, 11.

(4) Ma, Y.; Chen, C. T.; Meigs, G.; Randall, K.; Sette, F. *Phys. Rev. A* **1991**, *44*, 1848.

(5) Hitchcock, A. P.; Newbury, D. C.; Ishii, I.; Stohr, J.; Horsley, J. A.; Redwing, R. D.; Johnson, A. L.; Sette, F. *J. Chem. Phys.* **1986**, *85*, 4849.

(6) Outka, D. A.; Stöhr, J.; Rabe, J. P.; Swalen, J.; Rotermund, H. H. *Phys. Rev. Lett.* **1987**, *59*, 1321.

(7) Outka, D. A.; Stohr, J.; Rabe, J. P.; Swalen, J. D. *J. Chem. Phys.* **1988**, *88*, 4076.

(8) Hahner, G.; Kinzler, M.; Thummler, C.; Woll, C.; Grunze, M. *J. Vac. Sci. Technol., A* **1992**, *10*, 2758.

(9) Genzer, J.; Sivaniah, E.; Kramer, E. J.; Wang, J. G.; Korner, H.; Xiang, M. L.; Char, K.; Ober, C. K.; DeKoven, B. M.; Bubeck, R. A.; Chaudhury, M. K.; Sambasivan, S.; Fischer, D. A. *Macromolecules* **2000**, *33*, 1882.

(10) Stöhr, J.; Outka, D. A.; Baberscke, K.; Arvanitis, D.; Horsley, J. A. *Phys. Rev. B* **1987**, *36*, 2976.

(11) Schöll, A.; Fink, R.; Umbach, E.; Mitchell, G. E.; Urquhart, S. G.; Ade, H. *Chem. Phys. Lett.* **2003**, *370*, 834−841.

(12) Bagus, P. S.; Weiss, K.; Schertel, A.; Woll, C.; Braun, W.; Hellwig, C.; Jung, C. *Chem. Phys. Lett.* **1996**, *248*, 129.

(13) Weiss, K.; Bagus, P. S.; Wöll, C. *J. Chem. Phys.* **1999**, *111*, 6834.

(14) Ade, H.; Urquhart, S. NEXAFS Spectroscopy and Microscopy of Natural and Synthetic Polymers. In *Chemical Applications of Synchrotron Radiation*; Sham, T. K., Ed.; World Scientific Publishing: River Edge, NJ, 2002.

(15) Eberhardt, W.; Haelbich, R.-P.; Iwan, M.; Koch, E. E.; Kunz, C. *Chem. Phys. Lett.* **1976**, *40*, 180.

(16) Brown, F. C.; Bachrach, R. Z.; Bianconi, A. *Chem. Phys. Lett.* **1978**, *54*, 425.

(17) Bagus, P. S.; Krauss, M.; LaVilla, R. E. *Chem. Phys. Lett.* **1973**, *23*, 13.

(18) Kosugi, N. *J. Electron Spectrosc. Relat. Phenom.* **2004**, *137−140*, 335−343.

(19) Yates, B. W.; Hu, Y. F.; Tan, K. H.; Retzlaff, G.; Cavell, R. G.; Sham, T. K.; Bancroft, G. M. *J. Synchrotron Radiat.* **2000**, 296.

(20) Kosugi, N.; H., K. *Chem. Phys. Lett.* **1980**, *74*, 490.

(21) Kosugi, N.; Shigemasa, E.; Yagishita, A. *Chem. Phys. Lett.* **1992**, *190*, 481.

(22) Hunt, W. J.; Goddard, W. A. I. *Chem. Phys. Lett.* **1969**, *3*, 414.

(23) Frisch, M. J.; Trucks, G. W.; Schlegel, H. B.; Scuseria, G. E.; Robb, M. A.; Cheeseman, J. R.; Zakrzewski, V. G.; Montgomery, J. A., Jr.; Stratmann, R. E.; Burant, J. C.; Dapprich, S.; Millam, J. M.; Daniels, A. D.; Kudin, K. N.; Strain, M. C.; Farkas, O.; Tomasi, J.; Barone, V.; Cossi, M.; Cammi, R.; Mennucci, B.; Pomelli, C.; Adamo, C.; Clifford, S.; Ochterski, J.; Petersson, G. A.; Ayala, P. Y.; Cui, Q.; Morokuma, K.; Malick, D. K.; Rabuck, A. D.; Raghavachari, K.; Foresman, J. B.; Cioslowski, J.; Ortiz, J. V.; Stefanov, B. B.; Liu, G.; Liashenko, A.; Piskorz, P.; Komaromi, I.; Gomperts, R.; Martin, R. L.; Fox, D. J.; Keith, T.; Al-Laham, M. A.; Peng, C. Y.; Nanayakkara, A.; Gonzalez, C.; Challacombe, M.; Gill, P. M. W.; Johnson, B. G.; Chen, W.; Wong, M. W.; Andres, J. L.; Head-Gordon, M.; Replogle, E. S.; Pople, J. A. *Gaussian 98*, revision A.7; Gaussian, Inc.: Pittsburgh, PA, 1998.

(24) Huzinaga, S.; Andzelm, J.; Klobukowski, M.; Radzio-Andzelm, E.; Sasaki, Y.; tatewaki, H. *Gaussian Basis Sets for Molecular Orbital Calculations*; Elseview: Amsterdam, 1984.

(25) Kong, J.; White, C. A.; Krylov, A. I.; Sherrill, C. D.; Adamson, R. D.; Furlani, T. R.; Lee, M. S.; Lee, A. M.; Gwaltney, S. R.; Adams, T. R.; Ochsenfeld, C.; Gilbert, A. T. B.; Kedziora, G. S.; Rassolov, V. A.; Maurice, D. R.; Nair, N.; Shao, Y.; Besley, N. A.; Maslen, P. E.; Dombroski, J. P.; Daschel, H.; Zhang, W.; Korambath, P. P.; Baker, J.; Byrd, E. F. C.; Voorhis, T. V.; Oumi, M.; Hirata, S.; Hsu, C.-P.; Ishikawa, N.; Florian, J.; Warshel, A.; Johnson, B. G.; Gill, P. M. W.; Head-Gordon, M.; Pople, J. A. *J. Comput. Chem.* **2000**, *21*, 1532.

(26) Schirmer, J.; Trofimov, A. B.; Randall, K. J.; Feldhaus, J.; Bradshaw, A. M.; Ma, Y.; Chen, C. T.; Sette, F. *Phys. Rev. A.* **1993**, *47*, 1136.

(27) Herzberg, G. *Molecular Spectra and Molecular Structure II. Infrared and Raman Spectra of Polyatomic Molecules*; Prentice Hall: New York, 1945.

(28) Karlsen, T.; Leif J. Sæthre, L. J.; Brve, K. J.; Berrah, N.; Kukk, E.; Bozek, J. D.; Carroll, T. X.; Thomas, T. D. *J. Phys. Chem. A* **2001**, *105*, 7700.

(29) Saethre, L. J.; Svaeren O.; Svensson, S.; Osborne, S.; Thomas, T. D.; Jauhiainen, J.; Aksela, S. *Phys Rev. A.* **1997**, *55*, 2748.

(30) Rank, D. H.; Saksena, B. D.; Shull, E. R. *Discuss. Faraday Soc.* **1950**, *9*, 187.

(31) Tronc, M.; King, G. C.; Read, F. H. *J. Phys. B.* **1979**, *12*, 137.

(32) Wight, G. R.; Brion, C. E. *J. Electron Spectrosc. Relat. Phenom.* **1974**, *4*, 25.

(33) Kosugi, N. Molecular Inner Shell Spectroscopy. In *Chemical Applications of Synchrotron Radiation*; Sham, T. K., Ed.; World Scientific: Singapore, 2002.

(34) Gayles, J. N.; King, W. T. *Spectrochim. Acta* **1965**, *21*, 543.

(35) Snyder, R. G.; Schachtschneider, J. H. *Spectrochim. Acta* **1965**, *71*, 169.